



Nanoscale

Monolayer MoS₂ Growth at Au-SiO₂ Interface

Journal:	<i>Nanoscale</i>
Manuscript ID	NR-COM-06-2019-005119.R1
Article Type:	Communication
Date Submitted by the Author:	16-Aug-2019
Complete List of Authors:	Lim, Hong En; Tokyo Metropolitan University, Department of Physics Irisawa, Toshifumi; AIST Nanoelectronics Research Institute Okada, Naoya; AIST Nanoelectronics Research Institute Okada, Mitsuhiro; National Institute of Advanced Industrial Science and Technology Tsukuba Center Tsukuba Central, Nanomaterials Research Institute Endo, Takahiko; Tokyo Metropolitan University, Department of Physics Nakanishi, Yusuke; Tokyo Metropolitan University, Department of Physics Maniwa, Yutaka; Tokyo Metropolitan University, Department of Physics Miyata, Yasumitsu; Tokyo Metropolitan University

SCHOLARONE™
Manuscripts

COMMUNICATION

Monolayer MoS₂ Growth at Au-SiO₂ InterfaceHong En Lim,^{*a} Toshifumi Irisawa,^{*b} Naoya Okada,^b Mitsuhiro Okada,^c Takahiko Endo,^a Yusuke Nakanishi,^a Yutaka Maniwa^a and Yasumitsu Miyata^{*a}

Received 00th January 20xx,

Accepted 00th January 20xx

DOI: 10.1039/x0xx00000x

Atomically thin transition-metal dichalcogenides (TMDs) are attracting great interest for future electronic applications. Even though much effort has been devoted to preparing large-area, high-quality TMDs over the past few years, the samples are usually grown on substrate surfaces. Here, we demonstrate the direct growth of a MoS₂ monolayer at the interface between a Au film and a SiO₂ substrate. MoS₂ grains were nucleated below Au films deposited on SiO₂ via interface diffusion, and then grew into a continuous MoS₂ film. By programming the Au pattern deposited, controlled growth of MoS₂ with the desired size and geometry was achieved over preferred locations, facilitating its integration into functional field-effect transistors. Our findings elucidate the fabrication of a 2D semiconductor at the interface of bulk three-dimensional solids, providing a novel means for establishing a clean interface junction. It also offers a promising alternative to the site-selective synthesis of TMDs, that is expected to aid the fabrication of TMD-based nanodevices.

Following the successful production of monolayer carbon sheets (graphene), transition metal dichalcogenides (TMDs) became widely studied two-dimensional (2D) materials because of their electronic and optical properties at reduced dimensions.¹⁻³ TMDs possess layer-dependent band gaps and undergo strong optical interactions, making them highly promising candidates for next-generation semiconductor nanodevices.⁴⁻⁷ For the sake of scalability, bottom-up synthesis of atomically thin TMDs by chemical vapor deposition (CVD) was developed for large-area, high-quality growth of TMDs at

high yield.⁸⁻¹² Using such deposition methods, monolayers of TMDs are typically prepared on the exposed surface of a substrate. Fine tuning the various reaction parameters allows fabrication on a diverse range of substrates, with the most common being silicon dioxide (SiO₂),⁸⁻¹² gold (Au),^{13,14} graphene/graphite,^{15,16} and hexagonal boron nitride (*h*-BN).¹⁷⁻²⁰ Metal electrodes are then deposited on the TMD sheets to construct the desired device.

Nevertheless, materials prepared this way are inevitably exposed to surface adsorbates due to air and moisture. Storage under ambient conditions often results in rapid degradation²¹ or poor interface contact,^{22,23} requiring immediate use of the sample once it is removed from the reaction chamber. In addition, common device fabrication processes are potentially harmful. The TMD sheets may be contaminated by polymer residues during photoresist development or damaged by the bombardment of metal particles.²² Since the physical properties of such ultrathin materials are extremely sensitive to interface conditions, the effects can be detrimental. Moreover, despite advances in controlling crystal size and quality, TMD crystallites are generally distributed randomly on the substrates. The inability to manipulate their growth position has complicated circuit design and device integration. Thus, we have devoted our efforts to exploring other means of TMD synthesis that would facilitate controlled growth and direct device integration with a clean contact interface.

^a Department of Physics, Tokyo Metropolitan University, Hachioji, Tokyo 192-0397, Japan. E-mail: lim@tmu.ac.jp, ymiyata@tmu.ac.jp

^b Nanoelectronics Research Institute (NeRI), National Institute of Advanced Industrial Science and Technology (AIST), Tsukuba, Ibaraki 305-8568, Japan. E-mail: toshifumi1.irisawa@aist.go.jp

^c Nanomaterials Research Institute (NMRI), National Institute of Advanced Industrial Science and Technology (AIST), Tsukuba, Ibaraki 305-8565, Japan.

† Electronic Supplementary Information (ESI) available: [Topographic images of the MoS₂ sheet. Cross-sectional TEM images of the Au blocks taken after CVD reaction.]. See DOI: 10.1039/x0xx00000x

Here, we demonstrate the direct growth of highly uniform MoS₂ monolayers, a representative member of the TMD family, at the interface between Au films and SiO₂ substrates

created on the patterns to allow selective etching of the Au, forming gaps between the metal pads. This revealed the MoS₂ grown below, generating simple transistor devices for

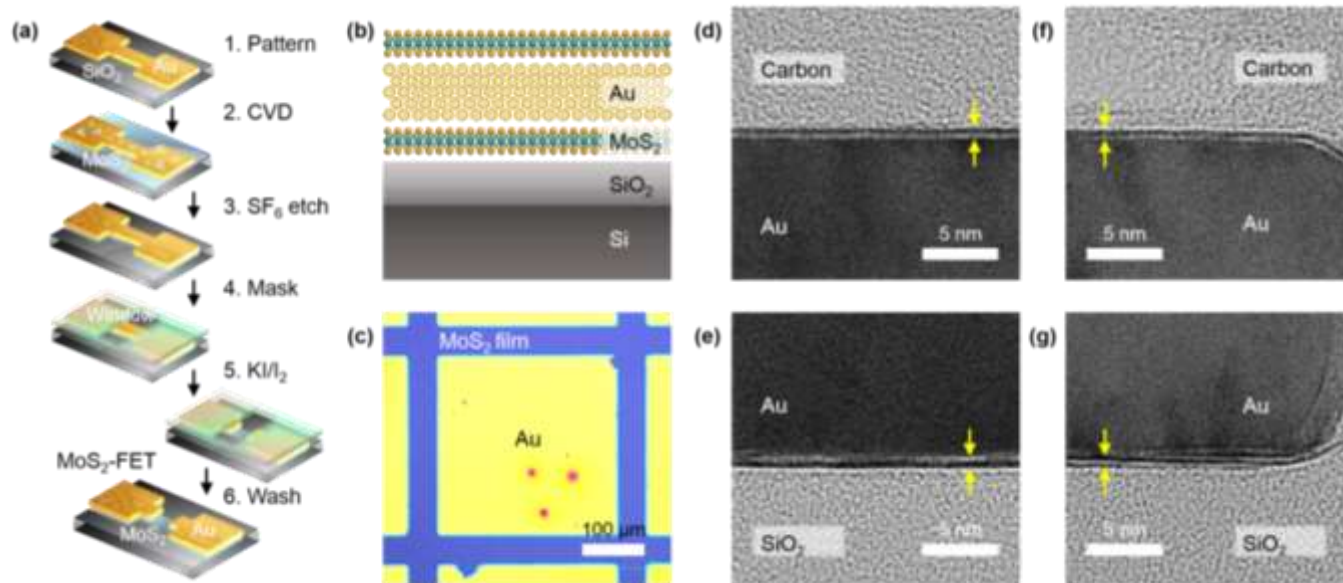


Fig. 1 Illustration of device fabrication and observations of interfacial-layer growth. (a) Schematic of device integration process: (i) metal deposition on substrate; (ii) CVD growth; (iii) surface MoS₂ removal; (iv) mask and window opening; (v) Au etching; and (vi) resist removal. (b) Cross-sectional schematic and (c) optical micrograph of a sample obtained by CVD growth. Cross-sectional TEM images taken from (d, e) the center and (f, g) edge regions of Au blocks, showing the MoS₂ grown (d, f) on top and (e, g) at the Au-SiO₂ interface.

by using a salt-assisted CVD method.^{11,24} The MoS₂ was generated via interface diffusion, forming a continuous monolayer film under predeposited Au. These MoS₂ layers have a crystal quality and optical properties comparable to exfoliated sheets. Field-effect transistors (FETs) with the desired geometry were fabricated by patterning the Au layer. With such interfacial growth, the MoS₂ layers are protected from interaction with the surrounding environment. Not only can a clean interface be established, but also sample degradation can be minimized, allowing long-term storage prior to use. Our findings show that it is possible to create a 2D layer at the interface between bulk 3D solids, which aid the simultaneous design, growth and integration of TMD-based nanodevices.

Results and discussion

The typical growth and device fabrication process flow is illustrated in Fig. 1a. In brief, first, Au patterns (thickness: 50 nm) were prepared on an oxidized silicon wafer by a standard photolithography and lift-off process. The substrate was then subjected to CVD in order to induce MoS₂ growth at the Au-SiO₂ interface. Next, SF₆ irradiation was performed to remove any MoS₂ that formed on the surfaces of the substrate and the Au film, leaving islands of sandwiched MoS₂ underneath. Finally, the substrate was spin-coated with a layer of photoresist, and windows of various sizes (5–100 μm) were

subsequent electrical probing and measurements.

Before proceeding to construct the FET devices described above, we tested the feasibility of interface growth by using a simple Au pattern. Figs. 1b and c show, respectively, a schematic and an optical image of a sample obtained by CVD using an Au-deposited substrate. As is frequently reported, this yielded a continuous MoS₂ monolayer in the channels between the Au pads on the bare substrate, judging by the optical contrast. MoS₂ monolayers were also formed on the Au surface, with a thickness of 6.5 Å, as shown in Figs. 1d and f.²⁵ In addition to this surface MoS₂, the cross-sectional TEM images in Figs. 1e and g reveal the presence of a layer-like structure at the Au-SiO₂ interface over the center and edge regions of the Au films. These correspond to MoS₂ layers that formed during CVD growth, as confirmed by the optical characterization presented below.

To confirm the composition of the material produced at the Au-SiO₂ interface, first, the surface MoS₂ was etched away, then, the Au was removed. Figs. 2a and b show, respectively, a schematic and an optical image of the sample prepared in step V of Fig. 1a after KI/I₂ treatment. A 20×50 μm film was observed when the top Au was dissolved, in agreement with the TEM observations. Raman measurements performed on this film yielded the spectrum in Fig. 2c. The characteristic in-plane vibrations of Mo and S atoms (E') and out-of-plane vibrations of S atoms (A'₁), signatures of MoS₂, are recorded at 385 and 405 cm⁻¹, respectively.^{26,27} The full width at half maximum (FWHM) of the E' peak is 3.8 cm⁻¹, suggesting a high

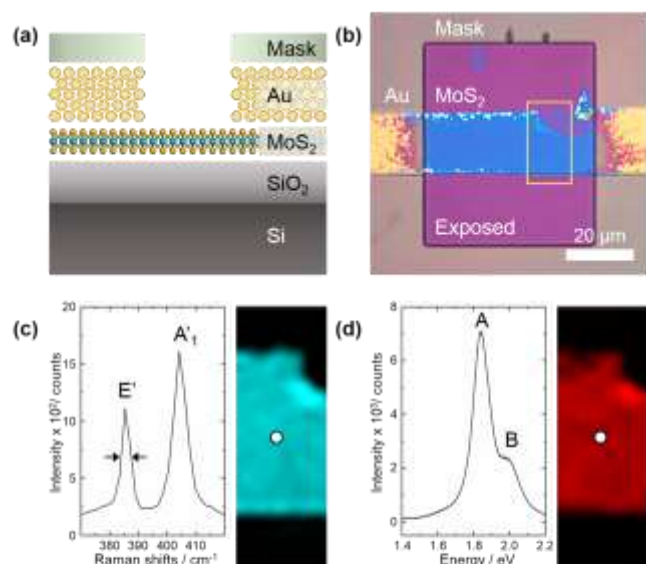


Fig. 2 Structural characterization. (a) Cross-sectional schematic and (b) optical micrograph of sample after Au etching in step V of Figure 1a. (c) Raman and (d) PL mapping images were obtained from the area outlined in (b). A FWHM of 3.8 cm^{-1} was registered for the E' peak. White dots indicate the positions at which the corresponding Raman and PL were taken.

crystal quality, comparable to that for surface-grown and exfoliated films.¹⁰ The separation of $\sim 20 \text{ cm}^{-1}$ between these peaks suggests the formation of a monolayer film.^{9,10} The photoluminescence (PL) spectrum for the synthesized MoS_2 sheet is shown in Fig. 2d. The A and B exciton peaks are at 1.8 and 2.0 eV, respectively, revealing an optical quality equivalent to that for an exfoliated monolayer.²⁸ It is also worth noting that the 2D sheet of MoS_2 fabricated in this manner exhibits exceptionally high uniformity in terms of both crystal quality and optical properties. The Raman and PL maps in Figs. 2c and d demonstrate a homogeneous distribution in the A'_1 and A exciton peak intensities for the area scanned, indicated in Fig. 2b. Further investigation into the surface morphology using atomic force microscopy (AFM) yielded the topographic images in Figs. S1a and b. A distinct, flat, continuous sheet is observed with a thickness of approximately 1 nm as shown in the topographic height profile in Fig. S1c.

The observation of such sandwiched MoS_2 is inspiring, as it may open up a new path for TMD growth and subsequent device integration via interface engineering, distinct from current techniques. Thus, it is crucial to know how growth can be initiated and how the thin sheet is generated. Fig. 3a shows an optical micrograph of a partially formed MoS_2 film, taken after Au removal. The corresponding topographic image is shown in Fig. 3b. As seen in these images, there are connected channels of MoS_2 along the side edges, with patches of MoS_2 grains having sizes of around 1–2 μm at the center. While this pointed to the polycrystalline nature of the synthesized film in Fig. 2, one may propose two plausible mechanisms whereby crystallization occurs: (i) the vapor-liquid-solid (VLS) growth model, where Mo and S atoms diffuse into the Au layer and

then precipitate out at the interface;²⁹ (ii) diffusion via the interface over the edges, i.e., the vapor-solid-solid (VSS) model.³⁰

Previous studies on Au-assisted surface MoS_2 growth suggest no signs of inclusion of Mo or S atoms into the Au core.^{25,31} The reaction with Au is restricted to the surface, where diffusion occurs solely at the outermost region forming the surface alloy. The reaction that proceeds at a much higher temperature than in previous studies may enhance the solubility and diffusion of these atoms into Au. However, the TEM images in Figs. 1d–g suggest otherwise. Rather than intermixing of the atoms inside bulk Au, a surface diffusion phenomenon was observed. A well-defined array of Au atoms with a lattice spacing of 2.4 Å, corresponding to Au (111) planes, is observed at the center of a layered sandwich structure. This array becomes less orderly at the Au– MoS_2 interface, indicating atomic diffusion at the Au surface.^{25,31} The absence of Mo or S inside bulk Au implies a different formation mechanism from the VLS model. Besides, the film structure of the deposited Au is well-preserved (Fig. 1c) with no microscopic pits observed (Fig. S2), indicating the stability of Au under the present reaction conditions. This rules out the possibility that diffusion may have taken place via channels generated by Au agglomeration.

The mechanism involved in such confined growth can be better comprehended through the optical images in Fig. 3c. They show the distribution of MoS_2 grains formed beneath Au blocks at various population densities over different regions of a substrate, which elucidate the process whereby a continuous film is eventually generated. Here, we observe a progressive increase in the number of grains, starting from the bordering edges moving towards the center. It is therefore evident at this stage that nucleation occurred via boundary diffusion, assuming VSS growth. While the boundary interface is known

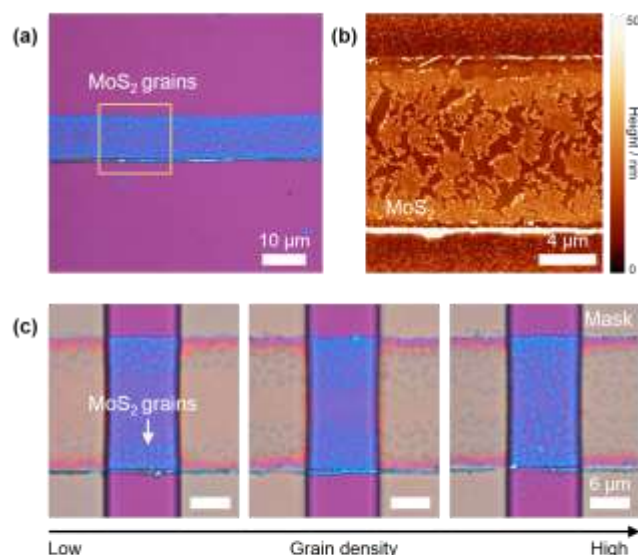


Fig. 3 Growth mechanism. (a) Optical and (b) topographic images of a partially formed MoS_2 film. Yellow rectangle shows the area where the image in (b) was taken. (c) Optical micrographs of MoS_2 grains ordered from low to high grain density.

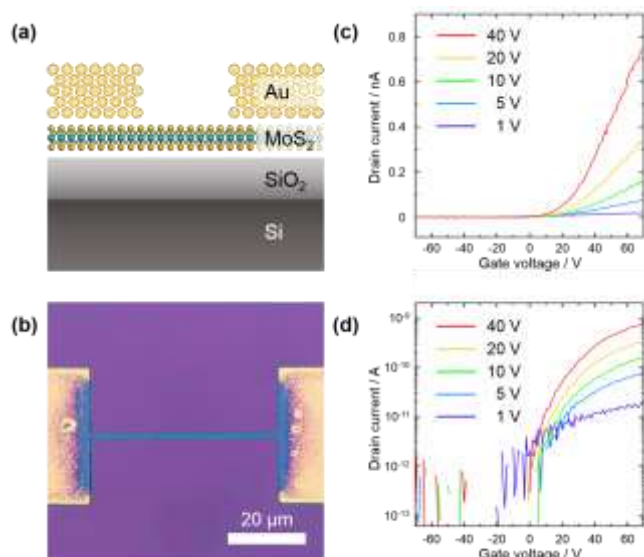


Fig. 4 MoS₂ field effect transistor (FET). (a) Schematic and (b) optical micrograph of a fabricated device. (c) Linear and (d) semi-logarithmic plots of the drain current, I_{ds} , versus the gate voltage, V_{gs} : transfer curves for one of the fabricated FET devices under various bias voltages: 40 V (red), 20 V (yellow), 10 V (green), 5 V (blue), and 1 V (violet).

to provide a good anchoring site for nucleation,²⁵ as evidenced by the connected channels formed along the edges (Figs. 3a, b), subsequent growth does not proceed merely through continual lateral elongation from these edges. Rather, a continuous MoS₂ film is generated through the coalescence of scattered grains as they grow, in a similar fashion to surface growth. The poor contact between Au and the SiO₂ surface³² is thought to play a major role in facilitating growth at the interface. Being a noble metal, Au with its low chemical reactivity tends to adhere only weakly to the substrate. It is common practice in the semiconductor industry to introduce metals such as Cr and Ti in order to improve the adhesion of Au films to the SiO₂ substrate.³³ Under high-temperature annealing, the interactions at the contact interface are substantially weakened, inducing an amplified gap. Hence the reactants can diffuse from the boundary interface, reach the center and become deposited as shown in Fig. 3c. These findings open up the opportunity for novel material synthesis via interface engineering.

As shown earlier in Fig. 1a, the present growth technique provides a useful means for simultaneously achieving site-specific synthesis and simple device fabrication. Figs. 4a and b show, respectively, a schematic and an optical micrograph of a fabricated FET. By patterning the deposited Au layer or the windows created for Au etching, the dimensions of the MoS₂ regions and the channel width of the device can be tailored with ease. Transfer curves (I_{ds} - V_{gs}) obtained for one of the present devices are plotted in Figs. 4c and d. Fig. 4c shows linear curves, whereas Fig. 4d shows semi-logarithmic plots for the FET obtained under various bias voltages, ranging from 1 to 40 V. A typical n-type behavior is observed: the drain

current increases with increasing applied gate voltage, in agreement with previous reports.^{4,8,10} For the device measured, we estimate an ON/OFF ratio of $\sim 10^3$.

Conclusions

We have demonstrated direct growth of a 2D MoS₂ sheet at the Au-SiO₂ interface. Monolayer grains of MoS₂ form beneath the Au film via interface diffusion, eventually merging into a continuous film. This offers a novel means for high-precision patterning of MoS₂, which enables simple integration of these 2D nanosheets into functional devices with sophisticated circuit designs. We believe that the method developed here can easily be extended to other growth techniques such as metal organic CVD^{34,35} and plasma-enhanced CVD,³⁶ which allow much lower growth temperatures to be used in the industry and are expected to lead to the fabrication of better flexible semiconductor devices. Our study not only offers a robust alternative for manipulating the growth of TMD materials, it also paves the way for the creation of other 2D materials at heterogeneous interfaces, as well as metal-semiconductor-insulator heterojunctions.

Experimental

Au patterning.

A series of 50-nm-thick Au patterns was prepared on a SiO₂/Si wafer by lift-off processes. Standard photolithography was used to define the patterns, and Au was deposited by either high-vacuum thermal evaporation or electron-beam evaporation. Lift-off was performed by dipping the samples into acetone.

CVD growth.

5 mg of KBr, 17 mg of MoO₃ (99% purity, Aldrich) and the Au-deposited SiO₂/Si substrate were loaded into a quartz boat and placed inside a quartz tube (1.5 cm in diameter, 6 cm in length). This tube was then inserted into a quartz chamber (3 cm in diameter, 100 cm in length) and set at the center of an electric furnace (ARF-30KC, Asahi Rika Manufacturing). An excess (~ 2 g) of S flakes ($\geq 99.99\%$ purity, Aldrich) was loaded into an alumina boat positioned 11 cm upstream from the edge of the furnace in the quartz chamber. The chamber was tightly sealed and purged with N₂ for 10 min. Next, the furnace temperature was gradually raised ($34\text{ }^\circ\text{C min}^{-1}$). Once it reached 720 °C, the ribbon heater was turned on to induce vaporization of S at 180 °C. The reaction lasted for 15 min at 740 °C. Immediately after this reaction, the system was cooled to room temperature. The flow of N₂ gas was maintained at 350 sccm throughout the experiment.

Device fabrication and electrical measurements.

The sample was subjected to SF₆ treatment to eliminate surface MoS₂. Next, windows of various lengths were created using photolithography. The Au in the exposed regions was subsequently removed using a gold etchant (Sigma-Aldrich) to

reveal the MoS₂ formed underneath. Finally, the photoresist mask was removed before measurements. All measurements were performed at room temperature under ambient pressure in a standard probe station.

Conflict of interest

There are no conflicts to declare.

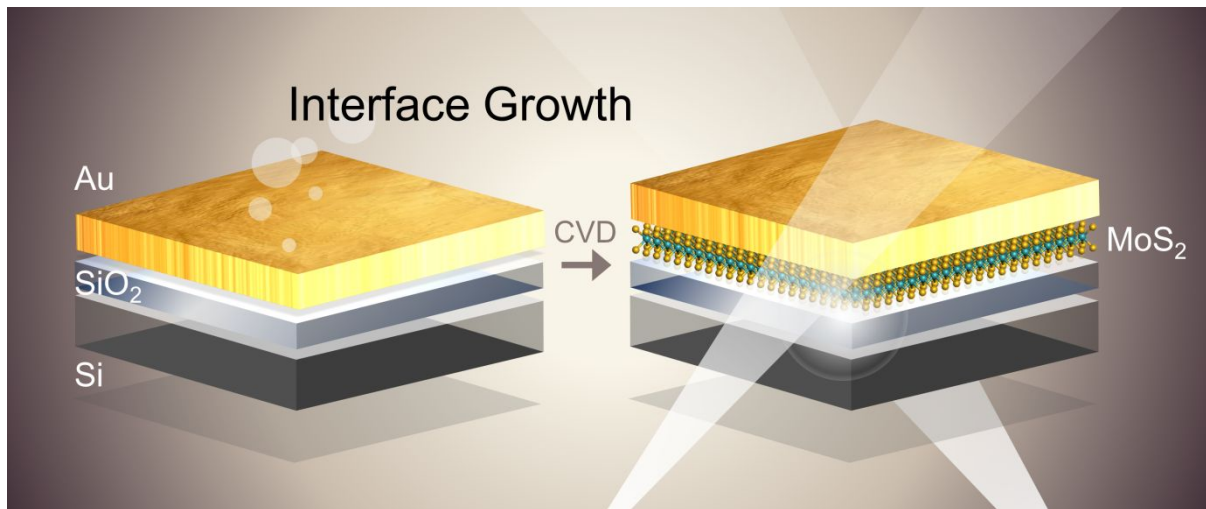
Acknowledgements

This work was supported by JST CREST (grant no. JPMJCR16F3), a Grant-in-Aid for Scientific Research (B) (no. JP18H01832, no. JP19H02543), and a Grant-in-Aid for Young Scientists (no. JP19K15393) from the Japan Society for the Promotion of Science (JSPS).

References

- Q. H. Wang, K. Kalantar-Zadeh, A. Kis, J. N. Coleman and M. S. Strano, *Nat. Nanotechnol.*, 2012, **7**, 699.
- F. Xia, H. Wang, D. Xiao, M. Dubey and A. Ramasubramaniam, *Nat. Photonics*, 2014, **8**, 899.
- K. F. Mak and J. Shan, *Nat. Photonics*, 2016, **10**, 216.
- B. Radisavljevic, A. Radenovic, J. Brivio, V. Giacometti and A. Kis, *Nat. Nanotechnol.*, 2011, **6**, 147.
- K. F. Mak, K. He, J. Shan and T. F. Heinz, *Nat. Nanotechnol.*, 2012, **7**, 494.
- K. F. Mak, K. L. McGill, J. Park and P. L. McEuen, *Science*, 2014, **344**, 1489-1492.
- W. Zheng, Y. Jiang, X. Hu, H. Li, Z. Zeng, X. Wang and A. Pan, *Adv. Opt. Mater.*, 2018, **6**, 1800420.
- Y.-H. Lee, X.-Q. Zhang, W. Zhang, M.-T. Chang, C.-T. Lin, K.-D. Chang, Y.-C. Yu, J. T.-W. Wang, C.-S. Chang, L.-J. Li and T.-W. Lin, *Adv. Mater.*, 2012, **24**, 2320-2325.
- Y. Zhan, Z. Liu, S. Najmaei, P. M. Ajayan and J. Lou, *Small*, 2012, **8**, 966-971.
- Y. Yu, C. Li, Y. Liu, L. Su, Y. Zhang and L. Cao, *Sci. Rep.*, 2013, **3**, 1866.
- S. Li, S. Wang, D.-M. Tang, W. Zhao, H. Xu, L. Chu, Y. Bando, D. Golberg and G. Eda, *Appl. Mater. Today*, 2015, **1**, 60-66.
- J. Zhou, J. Lin, X. Huang, Y. Zhou, Y. Chen, J. Xia, H. Wang, Y. Xie, H. Yu, J. Lei, D. Wu, F. Liu, Q. Fu, Q. Zeng, C.-H. Hsu, C. Yang, L. Lu, T. Yu, Z. Shen, H. Lin, B. I. Yakobson, Q. Liu, K. Suenaga, G. Liu and Z. Liu, *Nature*, 2018, **556**, 355-359.
- I. Song, C. Park, M. Hong, J. Baik, H.-J. Shin and H. C. Choi, *Angew. Chem. Int. Ed.*, 2014, **53**, 1266-1269.
- Y. Gao, Z. Liu, D.-M. Sun, L. Huang, L.-P. Ma, L.-C. Yin, T. Ma, Z. Zhang, X.-L. Ma, L.-M. Peng, H.-M. Cheng and W. Ren, *Nat. Commun.*, 2015, **6**, 8569.
- Y. Shi, W. Zhou, A.-Y. Lu, W. Fang, Y.-H. Lee, A. L. Hsu, S. M. Kim, K. K. Kim, H. Y. Yang, L.-J. Li, J.-C. Idrobo and J. Kong, *Nano Lett.*, 2012, **12**, 2784-2791.
- Y. Kobayashi, S. Sasaki, S. Mori, H. Hibino, Z. Liu, K. Watanabe, T. Taniguchi, K. Suenaga, Y. Maniwa and Y. Miyata, *ACS Nano*, 2015, **9**, 4056-4063.
- S. Wang, X. Wang and J. H. Warner, *ACS Nano*, 2015, **9**, 5246-5254.
- S. Zhao, T. Hotta, T. Koretsune, K. Watanabe, T. Taniguchi, K. Sugawara, T. Takahashi, H. Shinohara and R. Kitaura, *2D Materials*, 2016, **3**, 025027.
- M. Okada, Y. Miyauchi, K. Matsuda, T. Taniguchi, K. Watanabe, H. Shinohara and R. Kitaura, *Sci. Rep.*, 2017, **7**, 322.
- Y. Uchida, S. Nakandakari, K. Kawahara, S. Yamasaki, M. Mitsuhara and H. Ago, *ACS Nano*, 2018, **12**, 6236-6244.
- J. Gao, B. Li, J. Tan, P. Chow, T.-M. Lu and N. Koratkar, *ACS Nano*, 2016, **10**, 2628-2635.
- Y. Liu, J. Guo, E. Zhu, L. Liao, S.-J. Lee, M. Ding, I. Shakir, V. Gambin, Y. Huang and X. Duan, *Nature*, 2018, **557**, 696-700.
- Y. Wang, J. C. Kim, R. J. Wu, J. Martinez, X. Song, J. Yang, F. Zhao, A. Mkhoyan, H. Y. Jeong and M. Chhowalla, *Nature*, 2019, **568**, 70-74.
- K. Kojima, H. E. Lim, Z. Liu, W. Zhang, T. Saito, Y. Nakanishi, T. Endo, Y. Kobayashi, K. Watanabe, T. Taniguchi, K. Matsuda, Y. Maniwa, Y. Miyauchi and Y. Miyata, *Nanoscale*, 2019, DOI: 10.1039/C9NR01481K.
- Y. Li, S. Hao, J. G. DiStefano, A. A. Murthy, E. D. Hanson, Y. Xu, C. Wolverton, X. Chen and V. P. Dravid, *ACS Nano*, 2018, **12**, 8970-8976.
- C. Lee, H. Yan, L. E. Brus, T. F. Heinz, J. Hone and S. Ryu, *ACS Nano*, 2010, **4**, 2695-2700.
- H. Li, Q. Zhang, C. C. R. Yap, B. K. Tay, T. H. T. Edwin, A. Olivier and D. Baillargeat, *Adv. Funct. Mater.*, 2012, **22**, 1385-1390.
- A. Splendiani, L. Sun, Y. Zhang, T. Li, J. Kim, C.-Y. Chim, G. Galli and F. Wang, *Nano Lett.*, 2010, **10**, 1271-1275.
- S. Li, Y.-C. Lin, W. Zhao, J. Wu, Z. Wang, Z. Hu, Y. Shen, D.-M. Tang, J. Wang, Q. Zhang, H. Zhu, L. Chu, W. Zhao, C. Liu, Z. Sun, T. Taniguchi, M. Osada, W. Chen, Q.-H. Xu, A. T. S. Wee, K. Suenaga, F. Ding and G. Eda, *Nat. Mater.*, 2018, **17**, 535-542.
- S. Wu, C. Huang, G. Aivazian, J. S. Ross, D. H. Cobden and X. Xu, *ACS Nano*, 2013, **7**, 2768-2772.
- I. Song and H. C. Choi, *Chem. Eur. J.*, 2019, **25**, 2337-2344.
- R. Sangiorgi, M. L. Muolo, D. Chatain and N. Eustathopoulos, *J. Am. Ceram. Soc.*, 1988, **71**, 742-748.
- M. Todeschini, A. Bastos da Silva Fanta, F. Jensen, J. B. Wagner and A. Han, *ACS Appl. Mater. Interfaces*, 2017, **9**, 37374-37385.
- K. Kang, S. Xie, L. Huang, Y. Han, P. Y. Huang, K. F. Mak, C.-J. Kim, D. Muller and J. Park, *Nature*, 2015, **520**, 656.
- Y. Kobayashi, S. Yoshida, M. Maruyama, H. Mogi, K. Murase, Y. Maniwa, O. Takeuchi, S. Okada, H. Shigekawa and Y. Miyata, *ACS Nano*, 2019, **13**, 7527-7535.
- C. Ahn, J. Lee, H.-U. Kim, H. Bark, M. Jeon, G. H. Ryu, Z. Lee, G. Y. Yeom, K. Kim, J. Jung, Y. Kim, C. Lee and T. Kim, *Adv. Mater.*, 2015, **27**, 5223-5229.

Table of Contents Entry



Monolayer MoS₂ was grown directly at the interface between Au and SiO₂ by CVD.

(One sentence of text, maximum 20 words)